Analyses of low energy $\pi^+-{}^{12}$C, ^{16}O elastic scattering data using inverse scattering theory and suggested scaling method

Zuhair F. Shehadeh and Reham M. El-Shawaf
Physics Department, Taif University, Taif, Zip Code 21974, Saudi Arabia.
e-mail: zfs07@hotmail.com

Received 28 March 2016; accepted 27 May 2016

The elastic scattering data for low-energy ($T_\pi \leq 80$ MeV) positive pions from carbon-12 and oxygen-16 nuclei has been successfully analyzed by using our local optical potential based on the inverse scattering theory within the framework of the full Klein-Gordon equation. It is found that the same potential parameters used in the $\pi^-{-}^{12}$C, cases are still valid for $\pi^+{-}^{12}$C with a need to change the three parameters R_0, V_1 and W_3 with the pion's incident kinetic energy T_π. This is also found to hold in analyzing successfully the measured angular distributions for $\pi^+{-}^{16}$O in the same energy region. The systematic trends in the changed three free potential parameters R_0, V_1 and W_3 with T_π are compared to their counterparts for $\pi^+{-}^{12}$C. The different relations obtained for the two cases under consideration, $\pi^+{-}^{12}$C and $\pi^+{-}^{16}$O, reveals their dependence on the atomic weight of the target nucleus. As such, this suggests the use of a scaling method to obtain the potential parameters for a certain pion-nucleus system, as $\pi^+{-}^{16}$O, from a similar nearby one, as $\pi^+{-}^{12}$C. Further studies are needed to confirm our new findings.

Keywords: Pion-nucleus potential; Klein-Gordon equation; elastic scattering; inverse scattering theory; scaling method.

PACS: 25.80.Dj; 11.80.-m; 24.10.Ht

1. Introduction

It is well-known that pion-nucleus elastic scattering has been of great importance in nuclear physics and other related disciplines. The pion's properties of having a spin zero, an isospin one and a mass between the electron and the nucleon masses, make it the most useful probe of nuclear research [1]. Contrary to other probes, as electrons and protons, the pion has both charges which makes it special in describing Coulomb effects and studying the charge-exchange scattering experiments. In particular, low-energy pions are of special interest and importance as they can penetrate deeply into the nucleus, and information about the nuclear interior can be obtained [2]. This attribute is very important in gleaning nuclear information as nuclear structure and densities; in addition to other subtler aspects [3]. Nevertheless, the low-energy pion-nucleus elastic scattering process contributes to the solution of pionic-atom problem, especially the explanation of the shifts and widths of the energy levels in pionic atoms [4]. The significance of the low-energy pion-nucleus elastic scattering measurements remains incomplete without the complementary theoretical treatments. As alluded to in a previous study [5], several theoretical optical models, used in explaining the pion-nucleus elastic scattering data, faced a limited success. This provides a strong inducement to use our potential adopted in explaining successfully the measured differential and reaction cross sections for the elastically scattered low-energy negative pions from the same nucleus ^{12}C [6].

When phase shift analyses are available for elastically scattered pions from certain nuclei, one can use the inverse scattering theory as a guide to extract potential points from available phase shifts [7]. Then one can search for better potential parameters, by adjusting one parameter or more, that gives a reasonable agreement between the analytical forms of the potentials and the extracted potential points. This will be in conjunction with providing a nice explanation for the experimental angular distributions. The accuracy of the extracted potential points is affected by errors that obligatory exist in the phase shift analysis of the scattering data, and usually given as error bars. Alam [8] has highlighted all possible errors and provided valuable suggestions for reducing, but not eliminating, their effects.

So either the nonexistence of phase shift analysis or the unavoidable errors in the available phase shifts for pion-nucleus scattering data limits, if not prevents, the use of the inverse scattering theory. This creates a strong motivation to search for an alternative method that gives approximate values, if not exact ones, for the potential parameters. For nucleus-nucleus and alpha-nucleus cases, the scaling method [9] has shown a reasonable success. With this in mind, we are trying to test the extent of success for a scaling method, or relatively a similar one, in obtaining approximate values for the potential parameters by scaling from one pion-nucleus system to another nearby one in the same energy region. In this investigation, we try this method in obtaining the $\pi^+{-}^{16}$O potential parameters from the $\pi^+{-}^{12}$C potential parameters.

The following section briefs the theory. In its subsequent section, results and discussions for $\pi^+{-}^{16}$O and $\pi^+{-}^{12}$C systems, and the scaling method are outlined. The last section summarizes the conclusions.

2. Theory

The adopted nuclear potential here, $V_N(r)$, has the same analytical form used in our recent study [6]:

TABLE I. The changed three potential parameters R_0(in fm), V_1(in MeV) and W_3(in MeV) used in Eq. (1) for incident positive pions with energies T_π(in MeV) noted in column one and incident on carbon-12 target. Other potential parameters, also given in Eq. (1), are kept fixed with the values $V_0 = -37.0$ MeV, $a_0 = 0.324$ fm, $R_1 = 3.00$ fm, $a_1 = 0.333$ fm, $R_3 = 1.70$ fm and $a_3 = 0.370$ fm. Our calculated reaction cross sections, σ_r (theor) in millibarns, compared to the available experimental ones, σ_r(exp t) in millibarns, are listed in columns 5 and 6, respectively. The last column shows the references for available σ_r(exp t).

T_π	R_0	V_1	W_3	σ_r (theor)	σ_r (exp t)	References
13.9	4.11	160	-285.0	368.1	Not Available	-
20.0	4.00	150	-210.0	247.0	Not Available	-
30.0	3.85	129	-120.0	144.4	114	[4]
					94 ± 7	[30]
35.0	3.80	119	-95.0	119.1	Not Available	-
40.0	3.75	103	-77.0	106.5	Not Available	-
					125 ± 14	[29]
50.0	3.67	83	-53.0	83.4	117	[27]
					120.9 - 165.7	[28]
					152 ± 14	[29]
60.0					Not Available	
65.0	3.54	57	-54.0	99.1	202 ± 17	[29]
80.0	3.46	31	-95.0	158.7	Not Available	-

TABLE II. The changed three potential parameters R_0(in fm), V_1(in MeV) and W_3(in MeV) used in Eq. (1) for incident positive pions with energies T_π(in MeV) noted in column one and incident on oxygen-16 target. Other potential parameters, given in Eq. (1), are kept fixed with the same values as carbon-12 target, *i.e.* $V_0 = -37.0$ MeV, $a_0 = 0.324$ fm, $R_1 = 3.00$ fm, $a_1 = 0.333$ fm, $R_3 = 1.87$ fm and $a_3 = 0.370$ fm. Our calculated reaction cross sections, σ_r (theor) in millibarns, compared to the experimental ones, σ_r(exp t) in millibarns, are presented in columns 5 and 6, respectively. The last column displays the references for available σ_r(exp t).

T_π	R_0	V_1	W_3	σ_r (theor)	σ_r (exp t)	References
20.0	4.15	180	-300.0	352.9	Not Available	-
30.0	4.00	155	-175.0	211.5	44	[31]
40.0	3.89	125	-110.0	151.1	141	[31]
50.0	3.79	100	-78.0	122.1	184	[31]
					201	[4]
60.0	3.67	85	-54.0	92.5	Not Available	-
70.0	3.60	64	-80.0	143.4	Not Available	-
80.0	3.55	42	-133.0	223.2	Not Available	-

$$V_N(r) = \frac{V_0}{1+\exp\left(\frac{r-R_0}{a_0}\right)} + \frac{V_1}{\left[1+\exp\left(\frac{r-R_1}{a_1}\right)\right]^2} + i\frac{W_3\exp\left(\frac{r-R_3}{a_3}\right)}{\left[1+\exp\left(\frac{r-R_3}{a_3}\right)\right]^2} \quad (1)$$

i.e., it consists of a real part composed of an attractive Woods-Saxon and a repulsive squared Woods-Saxon terms, and an imaginary phenomenological attractive surface Woods-Saxon term, respectively. For an incident positive pion and a target nucleus, which is considered of a uniformly charged spherical distribution, the Coulomb potential term $V_C(r)$ is given by:

$$V_C(r) = \begin{cases} \frac{+Z_T e^2}{8\pi\varepsilon_0 R_c}\left(3-\frac{r^2}{R_c^2}\right) & r \le R_c \\ \frac{+Z_T e^2}{4\pi\varepsilon_0 r} & r > R_c \end{cases} \quad (2)$$

where Z_T is the atomic number of the target nucleus, $e^2/4\pi\varepsilon_0 = 1.44$ MeV.fm, ε_0 is the permittivity of free space and R_c is the Coulomb radius. The total potential $V(r)$ is the sum of nuclear and Coulomb potential terms:

$$V(r) = V_N(r) + V_C(r) \quad (3)$$

To calculate the scattering amplitude, the differential and reaction cross sections, the potential $V(r)$ is implemented in

the radial part of Klein-Gordon equation:

$$\left[d^2/dr^2 + k^2 - U(r) - \frac{l(l+1}{r^2}\right] R_{nl}(r) = 0 \qquad (4)$$

In order to put Eq. (4) in a more convenient mathematical form, $R_{nl}(r)$ is written as:

$$R_{n\ell}(r) = (kr)^{\ell+1}\varphi_{nl}(r) \qquad (5)$$

which assures the convergence of $\varphi_{nl}(r)$ at the origin, *i.e.* $\lim_{r\to 0}\varphi_{nl}(r) = 0$, and Eq. (4) becomes,

$$\left[\frac{d^2}{dr^2} + \frac{2(\ell+1)}{r}\frac{d}{dr} + k^2 - U(r)\right]\varphi_{nl}(r) = 0 \qquad (6)$$

with k^2 and $U(r)$ are given by

$$k^2 = (E^2 - m^2c^4)/\hbar^2c^2 \qquad (7)$$

$$U(r) = \frac{2E}{\hbar^2c^2}[V8r) - V^2(r)/2E] \qquad (8)$$

where E, m, and c are the effective pion energy, effective pion mass, and the velocity of electromagnetic wave in vacuum, respectively. Using Numerov's method, Eq. (4) is integrated numerically from the origin outward. As such the logarithmic derivative for the inner solution is obtained at the surface, *i.e.* at $r = R$ where the nuclear part of the potential $V_N(r)$ vanishes. In contrast, the outer solution, *i.e.* for $r \geq R$, where the potential is purely Coulomb, is well-known and is given by

$$\varphi_{n\ell}(r) = \frac{1}{(kr)^{\ell+1}}\Bigg\{F_\ell(\eta, kr) + \frac{\exp(2i\delta_\ell) - 1}{2i} \times \left[G_\ell(\eta, kr) + iF_\ell(\eta, kr)\right]\Bigg\} \qquad (9)$$

where the relativistic versions of the regular and irregular Coulomb wave functions, F_ℓ and G_ℓ respectively, are used. These relativistic Coulomb wave functions are generated when the nuclear part is turned off in solving the radial part of Klein-Gordon equation [10,11]. For a projected positive pion, the Sommerfeld parameter η is the defined by :

$$\eta = \frac{Z_T\alpha E}{k} \qquad (10)$$

with α is the fine structure constant.

At the matching radius $r = R$, which is taken 5.4 fm and 6.0 fm for $\pi^+-{}^{12}$C and $\pi^+-{}^{16}$O, respectively, the inner and outer logarithmic derivatives are equated and complex phase shifts, δ_ℓ, for all contributing partial waves, ℓ, are obtained. This makes it feasible to calculate the scattering amplitude $f(\theta)$, at angle θ in the center of mass system, using the formula:

$$f(\theta) = \frac{1}{2ik}\sum_{\ell=0}^{\infty}(2\ell+1)e^{2i\sigma_\gamma}[e^{2i\delta_\ell} - 1]P_\ell(\cos\theta) \qquad (11)$$

where $P_\ell(\cos\theta)$ is the Legendre polynomial, and σ_γ is the Coulomb phase shift defined by [12]:

$$\sigma_\gamma = \arg\Gamma\left(\gamma + \frac{1}{2} + i\eta\right) + \frac{1}{2}\pi\left(\gamma - \frac{1}{2} - \ell\right) \qquad (12)$$

and the parameter γ is given by :

$$\gamma = \sqrt{\left(\ell + \frac{1}{2}\right)^2 - Z_T^2\alpha^2} \qquad (13)$$

Knowing $f(\theta)$, the elastic differential cross section, $d\sigma/d\Omega$, can be calculated using the formula:

$$\frac{d\sigma}{d\Omega} = |f(\theta)|^2 \qquad (14)$$

In addition, one can easily calculate the reaction cross sections, σ_r, defined as:

$$\sigma_r = \frac{\pi}{k^2}\sum_{\ell=0}^{\infty}(2\ell+1)[1 - |S_\ell|^2] \qquad (15)$$

where $S_\ell = e^{2i\delta_\ell}$ is the S-matrix.

Benefiting from pion-^{12}C, ^{16}O available phase shifts [13,14] and the use of inverse scattering theory, with a complete relativistic treatment, in conjunction with obtaining a nice fit for available differential and reaction cross sections data within the framework of the relativistic Klein-Gordon equation, the real and imaginary parameters of the potentials were determined. The inverse scattering theory, used as a guide for extracting potential points from available phase shifts, was fully explained [15] and, as such, will not be repeated here.

3. Results and Discussion

3.1. $\pi^+-{}^{12}$C Case

In a recent study [6] the $\pi^--{}^{12}$C elastic scattering data has been successfully analyzed by using a three-term simple local optical potential obtained by using inverse scattering theory, as a guide, from available phase shifts. As such, and following the same strategy, we started by analyzing the $\pi^+-{}^{12}$C elastic scattering data in the same low-energy region. As indicated in Table I, six potential parameters, $V_0 = -37.0$ MeV, $a_0 = 0.324$ fm, $R_1 = 3.00$ fm, $a_1 = 0.333$ fm, $R_3 = 1.70$ fm and $a_3 = 0.370$ fm, were kept fixed and the other three parameters, R_0, V_1 and W_3, were changed with the pion's incident kinetic energy, T_π, to provide a nice agreement between measured and calculated differential and reaction cross sections. The analytical forms of these potentials, along with the extracted potential points from available phase shifts [13,16] are shown in Fig. 1 at all energies considered herein. In Fig. 2, and by using these potentials, our calculated differential cross sections are compared with the experimental ones [16-24]. The agreements are very satisfactory. In

addition, our calculated reaction cross sections at all energies under consideration, compared to the available experimental ones, are shown in Table I. Unfortunately, the available experimental and theoretical reaction cross sections [4,25-28] are cloudy and uncertain; and even with no agreement on their increasing behavior with energy [29]. In addition, the situation is more corrupted if one compares the reported reaction cross sections at 30 MeV [4,30,31] shown in Tables I and II as the value for the carbon case is almost two to three times as that for the oxygen case.

Unfortunately this is an outrageous contradiction, but still acceptable compared to the more valuable and positive results. As such, the priority here is given for the ability of the potential to provide a nice agreement between predictions and experiment for elastic differential cross sections rather than reaction cross sections. In principle, this forms a stringent test for the correctness and success of the potential. Nevertheless, and in our investigation, one can also notice that the calculated reaction cross sections simulate the corresponding changes in the strength of the imaginary pat, W_3. This is highly expected as both represent the opening of inelastic channels.

Concerning the three potential parameters (R_0, V_1, W_3) that change with T_π, it is found that both R_0 and V_1 change linearly, while W_3 changes quadratically, with T_π as clearly represented in Figs. 6, 7 and 8. By applying a spline fit for each of these graphs, the following corresponding relations are obtained:

$$R_0 = -9.58 \times 10^{-3} T_\pi + 4.17 \quad \text{(fm)} \tag{16}$$

$$V_1 = 2.00 T_\pi + 187.00 \quad \text{(MeV)} \tag{17}$$

$$W_3 = -0.125 T_\pi^2 + 14.4 T_\pi - 451.0 \quad \text{(MeV)} \tag{18}$$

It is clear that the $V_1 - T_\pi$ relation in (17) is different from the corresponding one obtained for the $\pi^- - {}^{12}$C scattering

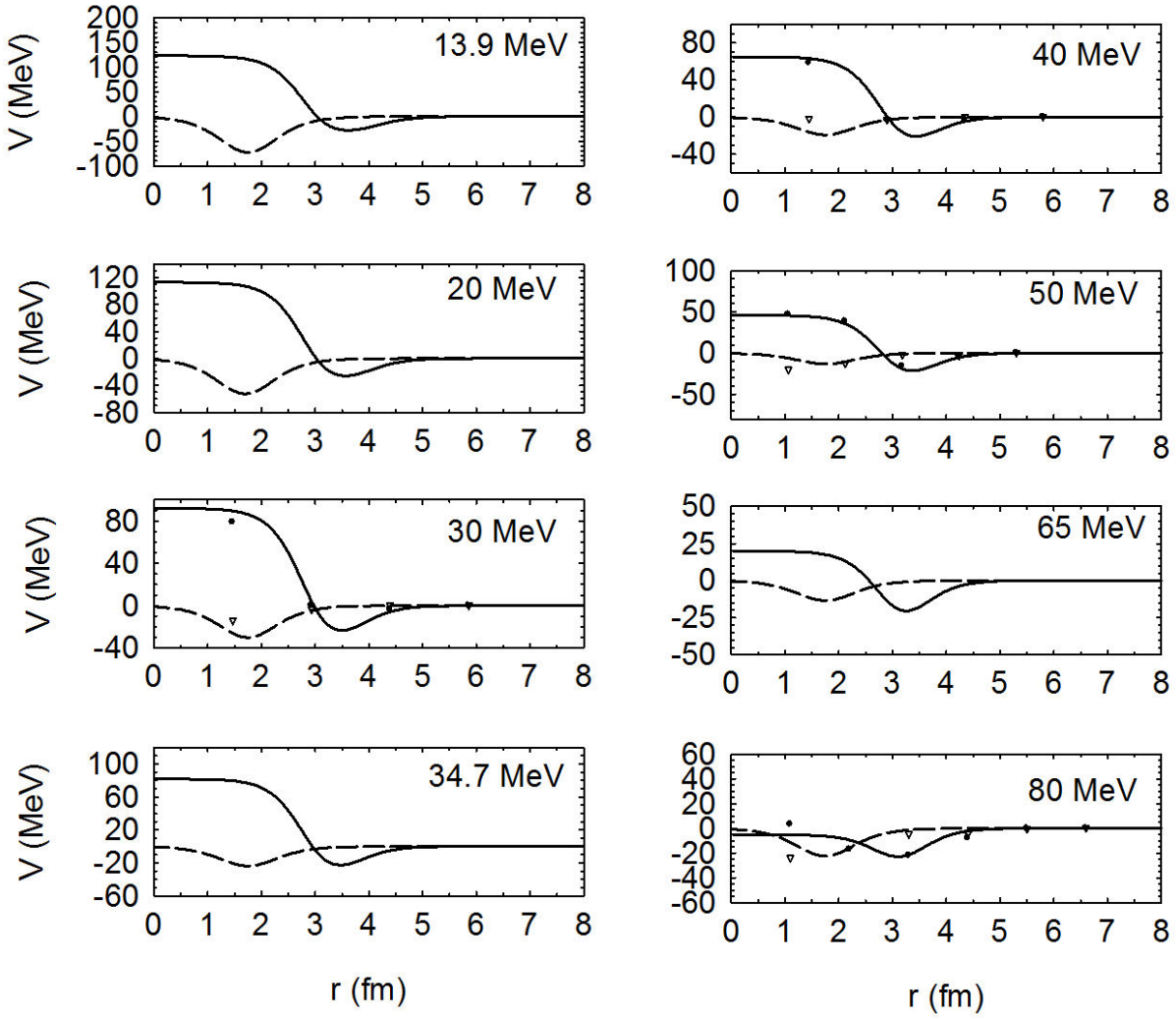

FIGURE 1. The real (solid line) and imaginary (dashed line) parts of the potentials used in analyzing $\pi^+ - {}^{12}$C elastic scattering data at the indicated eight pion's incident kinetic energies. Where available, the analytical forms of the real and imaginary parts of the potentials are compared with the real and imaginary potential points, shown as solid circles and empty triangles, respectively, extracted from available phase shifts [13,16] using inverse scattering theory.

case [6]. This consolidates the need for different, although close, potentials in explaining the elastic scattering data for pions with both charges. This is also supported by the obtained values, and the corresponding relations, for R_0 and W_3.

3.2. π^+-^{16}O Case

The success of our potential in explaining the π^+-^{12}C elastic scattering data forms an inducement to use it in analyzing the π^+-^{16}O. This has been carried out in a similar fashion as phase shift analyses are available at most, if not all, energies under consideration. This enables the use of the well-established inverse scattering theory, for the elastic scattering of two non-identical particles, to be used as a guide in determining the potential parameters. The obtained potential parameters consist of six fixed parameters with the values $V_0 = -37.0$ MeV, $a_0 = 0.324$ fm, $R_1 = 3.00$ fm, $a_1 = 0.333$ fm, $R_3 = 1.87$ fm and $a_3 = 0.370$ fm; and the three changed parameters R_0, V_1 and W_3. All these parameters are indicated in Table II. The analytical forms of the potentials, real and imaginary parts, are plotted in Fig. 3. These potentials, real and imaginary parts, are reasonably compared with the potential points, solid circles and empty triangles, respectively, extracted from available phase shifts [14,31] using inverse scattering theory. Using these potentials, with only three free parameters, our calculated differential cross sections are in very good agreement with the experimental values at 30, 40 and 50 MeV [16,20] but slightly differ at forward angles for 20 MeV [19] and at large angles for 80 MeV [1] as clearly depicted in Fig. 4. It is worth to mention that all the fixed six parameters have the same values as for π^+-^{12}C case, but with a slight change in the absorption radius R_3. As in the π^+-^{12}C case, our calculated reaction cross sections, compared to the experimental ones where available, are tabulated in Table II; and again the evidence

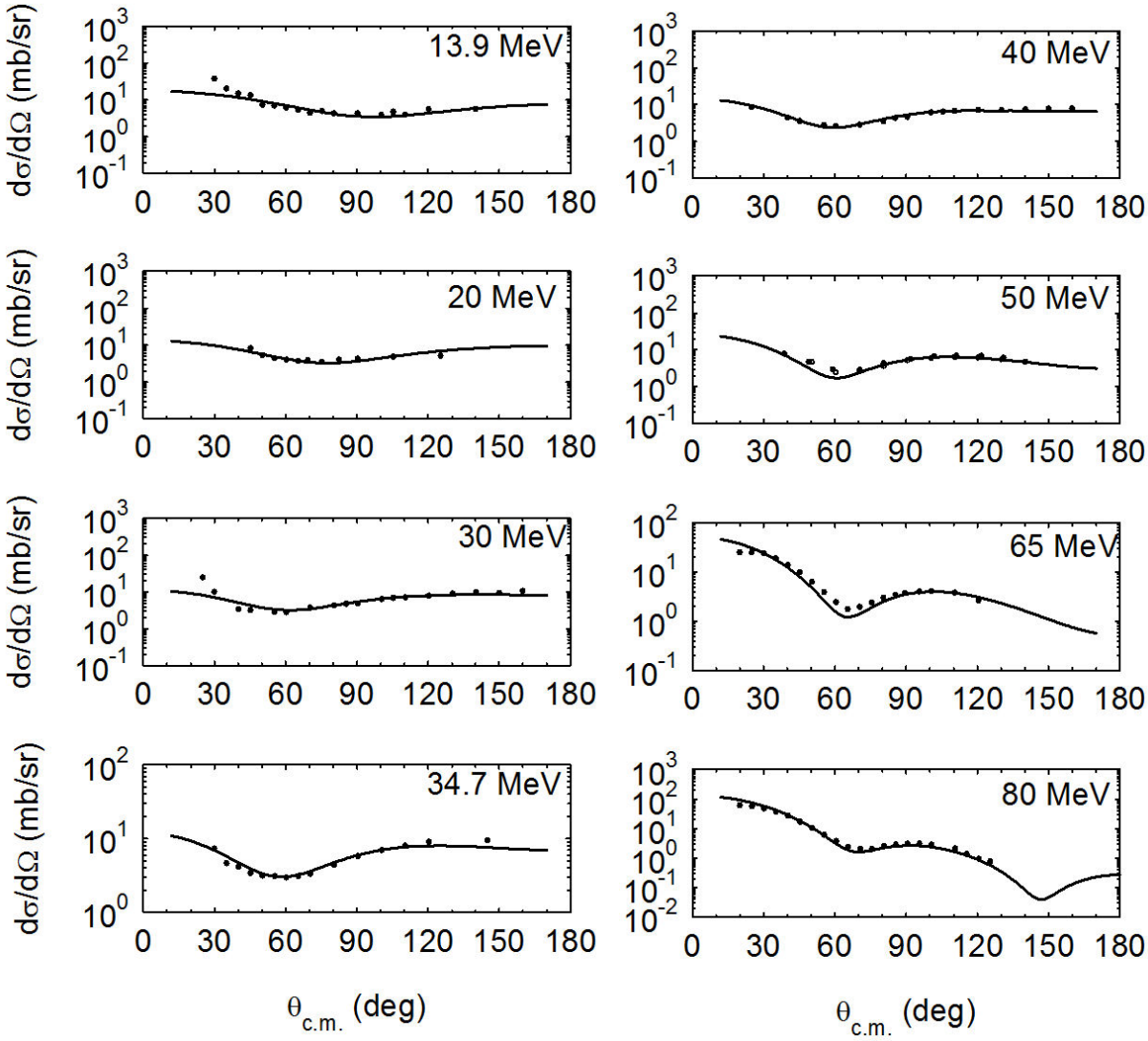

FIGURE 2. Our calculated differential cross sections represented by solid lines, using our potentials in Fig. 1, are compared with the measured ones [16-24] at the indicated eight pion's incident kinetic energies.

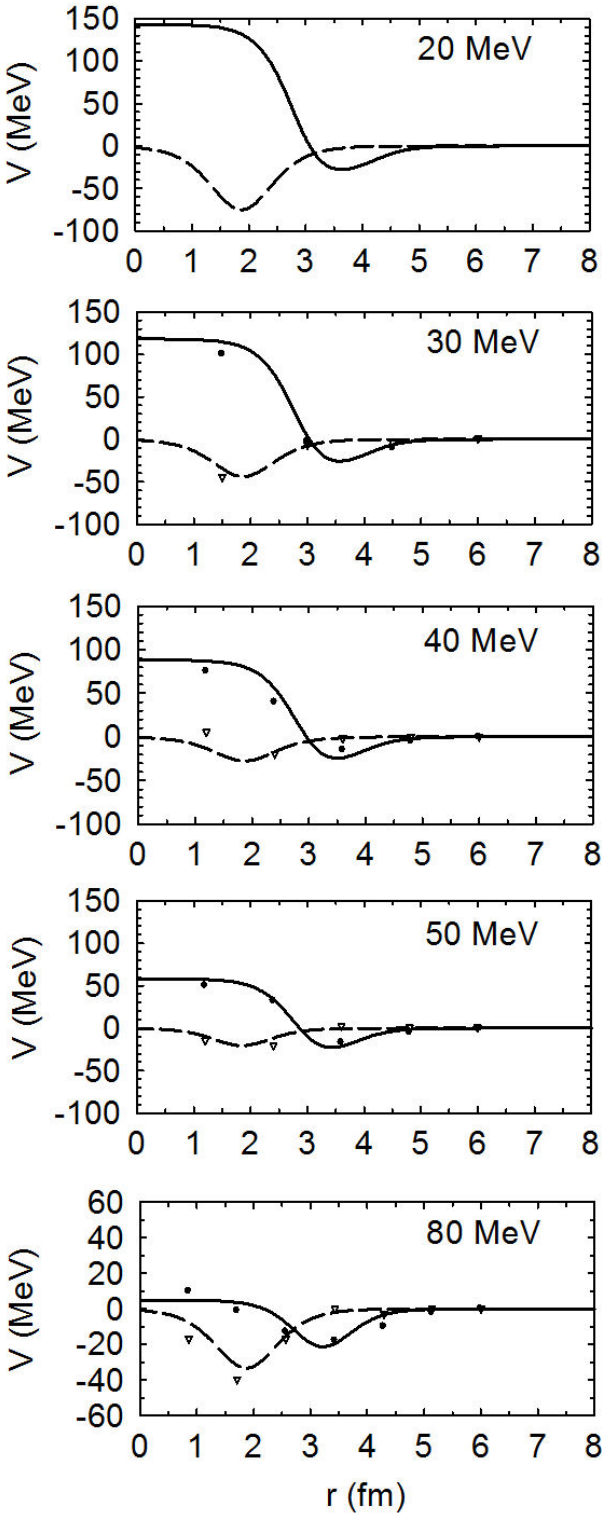

FIGURE 3. The real (solid line) and imaginary (dashed line) parts of the potentials used in analyzing $\pi^{+}-^{16}$O elastic scattering data at the indicated five pion's incident kinetic energies. The analytical forms of the real and imaginary parts of the potentials are compared with the real and imaginary potential points, shown as solid circles and empty triangles, respectively, extracted from available phase shifts [14,34] using inverse scattering theory.

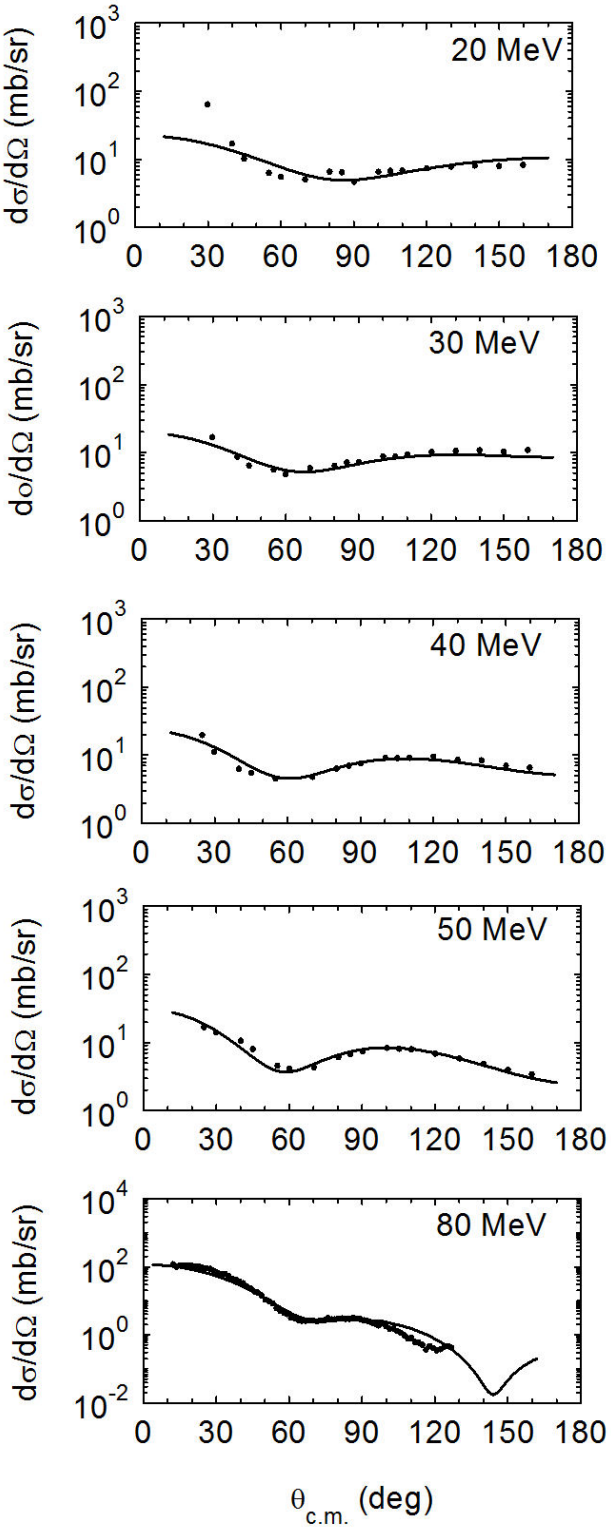

FIGURE 4. Our calculated differential cross sections represented by solid lines, using our potentials in Fig. 3, are compared with the measured ones at $T_\pi = 20$ MeV [19], $T_\pi = 30$, 40, 50 MeV [16,20] and $T_\pi = 80$ MeV [1] as indicated.

on available experimental and theoretical values [4,16,26,31] is scanty. This is very obvious in the very large discrepancy

in the total reaction cross sections of 166 and 284 mb, at 50 MeV for $\pi^+ - {}^{16}$O case, reported by Meirav *et al*. [26] and Malbrough *et al*. [31], respectively. Hence, our calculated reaction cross sections are proposed pending further related studies.

Again, applying a spline fit to each of the three changed parameters R_0, V_1 and W_3 with T_π reveals the following relations:

$$R_0 = -10.10 \times 10^{-3} T_\pi + 4.311 \quad \text{(fm)} \tag{19}$$

$$V_1 = -2.27 T_\pi + 221.00 \quad \text{(MeV)} \tag{20}$$

$$W_3 = -0.162 T_\pi^2 + 18.9 T_\pi - 607.0 \quad \text{(MeV)} \tag{21}$$

These three relations for $\pi^+ - {}^{16}$O case are different from their counterparts given by Eqs. (16), (17) and (18) for $\pi^+ - {}^{12}$C case. This strongly indicates the dependence of the parameters of these potentials on the atomic mass, A, of the target nucleus. So in comparison, and in connection, with the scaling method for none relativistic alpha-nucleus and nucleus-nucleus scattering cases, does a scaling method exist for pion-nucleus cases?

3.3. The Scaling Method

Scaling potential parameters of a certain nuclear system to another nearby one has been used with a reasonable success. It has been established that scaled potential parameters can predict the general feature of the cross section. It is worthwhile mentioning that the derived scaling relations rely on a strong theoretical background as they are connected to the well-known energy density functional (EDF) theory [7]. In fact, Haider and Malik [9] obtained the ^{12}C - ^{12}C potential parameters by scaling the ^{16}O - ^{16}O potential parameters [32]. Also Malik and Reichstein [33] have obtained the α - ^{32}S, ^{34}S potentials by scaling from the α - ^{28}Si potential parameters [34]. In addition, Shehadeh and his coworkers [7,35,36] have used the scaling procedure as a guide in determining the potential parameters for ^{32}S - ^{64}Ni, ^{36}S - ^{58,64}Ni, ^{40}Ca - ^{48}Ca and ^{27}Al - ^{58}Ni nuclear systems. Nevertheless, Sabra *et al*. [37] have used scaling to obtain the potential used in their study. In all mentioned cases, the goals behind using the obtained potentials by scaling procedure are achieved; and a remarkable success was very obvious. This

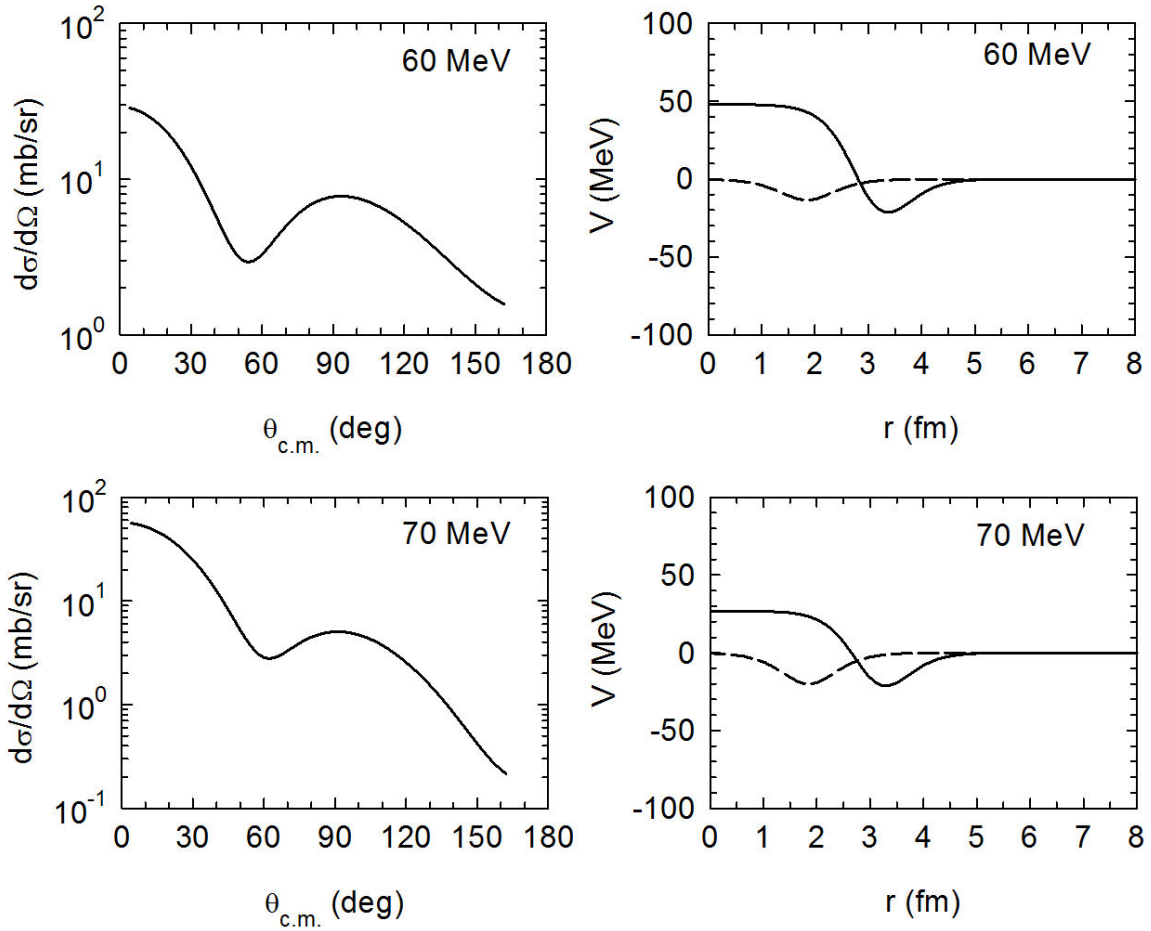

FIGURE 5. In the left side, predicted elastic differential cross sections calculated at pion's incident kinetic energies of 60 and 70 MeV. The right side shows the analytical forms of the potentials, real and imaginary represented by solid and dashed lines, respectively, used in predicting these elastic differential cross sections.

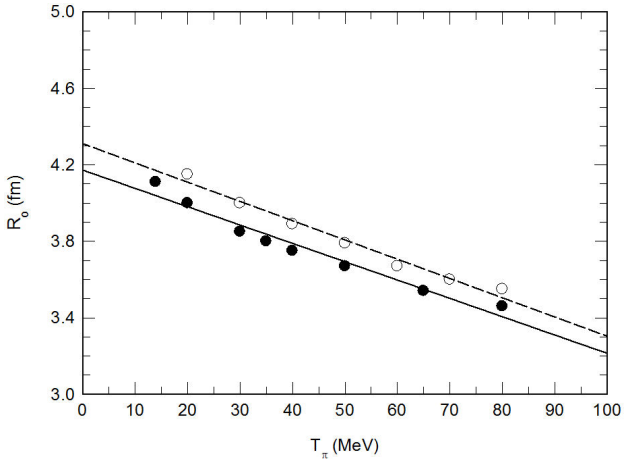

FIGURE 6. The radius of the real attractive Woods-Saxon potential term versus the pion's incident kinetic energy. The solid and dashed lines are for $\pi^+ - {}^{12}$C and $\pi^+ - {}^{16}$O cases, respectively.

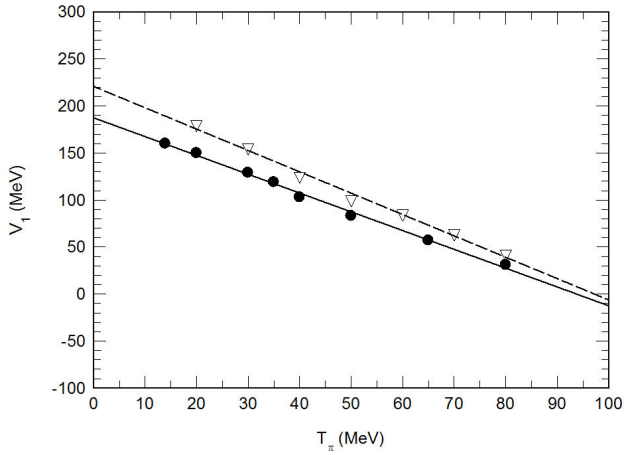

FIGURE 7. The height of the repulsive real potential term versus the pion's incident kinetic energy. The solid and dashed lines are for $\pi^+ - {}^{12}$C and $\pi^+ - {}^{16}$O cases, respectively.

is also compelling to use the scaling method in analyzing high-energy alpha-nucleus scattering data from a recent successful determined potential [11].

Here, and in this new preliminary study, we are investigating the possibility of scaling from one pion-nucleus system to another; namely from $\pi^+ - {}^{12}$C into $\pi^+ - {}^{16}$O. So far, we have obtained systematic trends for the changed potential parameters with energy rather than exact scaling relations. This is clearly indicated in the Figs. 6, 7 and 8. This is also legal as the possibility of parameterization of pion-nucleus optical potential has been previously drawn to attention [38].

One may notice that the fixed parameter R_3 has different values for oxygen-16, $R_3 = 1.87$ fm, and carbon-12, $R_3 = 1.70$ fm, cases. It is very interesting to see that the ratio, $1.87/1.70 \approx 1.1$, equals the ratio $A_2^{1/3}/A_1^{1/3} = (16)^{1/3}/(12)^{1/3}$. On the other hand R_1 is the same for both cases which may tell that the positive incident pion starts facing a noticeable repulsion at $R_1 = 3.0$ fm. This is legitimate as the two target nuclei are close to each other and each of them is tightly bound nucleus. For the parameter R_0, it decreases as T_π increases. The ratio between the slopes of R_0 given by the relations (16) and (19), and represented in Fig. 6, is 1.054. Similarly, the parameter V_1 also decreases as T_π increases. The ratio between the slopes of V_1 given in (17) and (20), and plotted in Fig. 7, is 1.135. Such close ratios which are, in turn, close to $(A_2)^{1/3}/(A_1)^{1/3} = 1.10$ makes it feasible to scale the two parameters R_0 and V_1 with the pion's incident kinetic energy T_π and the atomic weights, (A_1) and (A_2), of the two target nuclei in the two pion-nucleus systems. On the contrary, the parameter W_3 changes quadratically with T_π. A deep look at the W_3-relations, given in (18) and (21), reveals that relation (21) is obtained by multiplying (18) with 1.3 which is approximately the ratio between the atomic weights of the two target nuclei, *i.e.* 16/12, *i.e.* W_3 didn't follow the $A^{1/3}$ rule in scaling. Moreover, Fig. 8 shows that both $W_3 - T_\pi$ curves have a minimum at 60 MeV. Such a behavior is in accord with the calculated cross sections listed in the tables; and may be attributed to the pion mean free path that allows a minimal number of pion-nucleon inelastic scattering for $T_\pi = 60$ MeV compared to other lower and higher energies in the low energy region under consideration. This is clearly manifested in W_3 as the other two imaginary parameters, R_3 and a_3, remain unchanged.

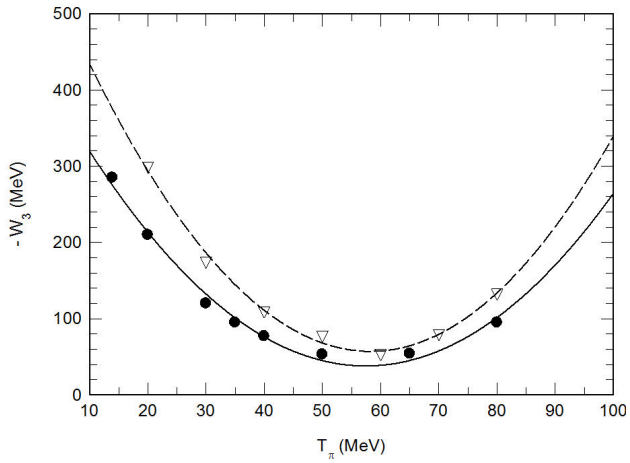

FIGURE 8. The depth of the imaginary part of the potential versus the pion's incident kinetic energy. The solid and dashed curves are for $\pi^+ - {}^{12}$C and $\pi^+ - {}^{16}$O cases, respectively.

In Fig. 6, the values of R_0 at 13.9 and 80 MeV are not on the straight line which may suggest that a better scaling procedure is obtained for a certain energy interval as $T_\pi < 20$ MeV, $20 \leq T_\pi \leq 80$ MeV and $80 \leq T_\pi \leq 100$ MeV. With a reasonable degree of confidence, especially in the energy region $20 \leq T_\pi < 80$ MeV, the new suggested scaling method is summarized by a) multiplying the two parameters R_0 and V_1 by 1.05-1.14, b) multiplying the parameter W_3 by 1.30, and c) keeping the other six parameters fixed with R_3 follows the $A^{1/3}$ rule. To become sure and more confident, and with these encouraging results, the analyses of elastically scattered positive pions from ^{28}Si, ^{232}S, ^{40}Ca, ^{56}Fe, ^{58}Ni and ^{90}Zr nuclear targets by scaling from $\pi^+ - {}^{12}$C and $\pi^+ - {}^{16}$O cases will be investigated in the nearest future.

4. Conclusions

In this investigation, the adopted simple local optical potential shows a remarkable success in explaining low-energy $\pi^+ - {}^{12}$C, ^{16}O elastic differential cross sections data. The role of the inverse scattering theory in guiding to the correct potential parameters is very obvious. For the first time, the use of a scaling method with changes in three free potential parameters R_0, V_1 and W_3 with T_π has been established. In fact, linear relations for R_0 and V_1, and quadratic relations for W_3 for both $\pi^+ - {}^{12}$C and $\pi^+ - {}^{16}$O systems have been obtained. The slopes of R_0 and V_1 are related to $(A_2)^{1/3}/(A_1)^{1/3}$ while W_3 is connected to A_2/A_1. Also the ratio between R_3 values for $\pi^+ - {}^{12}$C and $\pi^+ - {}^{16}$O cases is found to be the same as $(A_2)^{1/3}/(A_1)^{1/3}$ and, as such, to follow the $A^{1/3}$ rule. With these important findings, this paper will be a contribution to fit further experimental data in the energy range defined here, and shows the success of the scaling method prediction of potential parameters on similar nuclei to describe the pion plus elastic scattering.

Acknowledgments

One of the authors (ZFS) is very pleased to acknowledge the encouragement and financial support of the Deanship of Scientific Research at Taif University for carrying out this investigation. This paper is dedicated to the blessed soul of Prof. F.B. Malik who suggested this important new study.

1. J.P. Albanese *et al*., *Nucl. Phys. A* **350** (1980) 301-331.
2. V. Yu. Alexakhin *et al*., *Phys. Rev. C* **57** (1998) 2409-2415.
3. K.K. Seth *et al*., *Phys. Rev.* C **41** (1990) 2800-2808.
4. K. Stricker, H. McManus and J.A. Carr, *Phys. Rev. C* **19** (1979) 929-947.
5. Z.F. Shehadeh, *J. Assoc. Arab Univ. Basic Appl. Sci.* **14** (2013) 32-37.
6. Z.F. Shehadeh, *Journal of Modern Physics* **5** (2014) 1652-1661.
7. Z.F. Shehadeh, "*Non-relativistic nucleus-nucleus and relativistic pion-nucleus interactions*", Ph. D. Thesis Southern Illinois University at Carbondale, (1995).
8. M.M. Alam, "*Inverse scattering methods to determine potentials between two identical and nonidentical nuclei*", Ph. D. Thesis Southern Illinois University at Carbondale, (1991).
9. Q. Haider and F.B. Malik, *Phys. G: Nucl. Phys.* **7** (1981) 1661-1669.
10. R.A. Eisenstein and G.A. Miller, *Comp. Phys. Commun.* **8** (1974) 130-140.
11. Z.F. Shehadeh, *Turk. J. Phys.* **39** (2015) 199-207.
12. H.M. Pilkuhn, *Relativistic Particle Physics*, (Springer-Verlag, New York, 1979).
13. O. Dumbrajs, J. Fröhlich, U. Klein and H. G. Schlaile, *Phys. Rev. C* **29** (1984) 581-591.
14. J. Fröhlich, H.G. Schlaile, L. Streit and H.Z. Zingl, *Z. Phys. A-Atoms and Nuclei* **302** (1981) 89-94.
15. Z.F. Shehadeh, *Int. J. Mod. Phys. E* **18** (2009) 1615-1627.
16. M. Blecher *et al*., *Phys. Rev. C* **20** (1979) 1884-1890.
17. D.R. Gill *et al*., *Phys. Rev. C* **26** (1982) 1306-1309.
18. M. Hanna, *Low energy elastic scattering and the pionic atom anomaly*, M.S. Thesis University of British Columbia, (1988).
19. F.E. Obenshain *et al*., *Phys. Rev. C* **27** (1983) 2753-2758.
20. B.M. Preedom *et al*., *Phys. Rev. C* **23** (1981) 1134-1140.
21. J.F. Amann *et al*., *Phys. Rev. C* **23** (1981) 1635-1647.
22. R.J. Sobie *et al*., *Phys. Rev. C* **30** (1984) 1612-1621.
23. M. Blecher *et al*., *Phys. Rev. C* **28** (1983) 2033-2041.
24. M.J. Leitch *et al*., *Phys. Rev. C* **29** (1984) 561-568.
25. O. Meirav, E. Friedman, A. Altman, M. Hanna, R.R. Johnson and D.R. Gill, *Phys. Rev. C* **36** (1987) 1066-1073.
26. O. Meirav, E. Friedman, R.R. Johnson, R. Olszewski and P. Weber, *Phys. Rev. C* **40** (1989) 843-849.
27. M.A. Moinester *et al*., *Phys. Rev. C* **18** (1978) 2678-2682.
28. A.A. Ebrahim and S.A.E. Khallaf, *Acta Physica Polonica B* **36** (2005) 2071-2085.
29. A. Sanders *et al*., *Phys. Rev. C* **53** (1996) 1745-1752.
30. E. Friedman, A. Goldring, R.R. Johnson, O. Meirav, D. Vetterli and P. Weber, *Phys. Lett. B* **257** (1991) 17-20.
31. D.J. Malbrough *et al*., *Phys. Rev. C* **17** (1978) 1395-1401.
32. D.A. Bromley, J.A. Kuehner and E. Almquist, *Phys. Rev.* **123** (1961) 878-893.
33. F.B. Malik and I. Reichstein, *Proceedings of In 1st International Conference on Clustering Phenomena in Atoms and Nuclei* (Heidelberg, Germany) (1992) 126.
34. P. Manngard, M. Brenner, M.M. Alam, I. Reichstein and F.B. Malik, *Nucl. Phys. A* **504** (1989) 130-142.
35. A.V. Pozdnyakov, I. Reichstein, Z.F. Shehadeh and F.B. Malik, *Condensed Matter Theories* **10** (1995) 365-380.
36. Z.F. Shehadeh and F.B. Malik, *Bull. Am. Phys. Soc.* **36** (1991) 2116.
37. M.S. Sabra, Z.F. Shehadeh and F.B. Malik, *Eur. Phys. J. A* **27** (2006) 167-181.
38. L.C. Liu and C.M. Shakin, *Phys. Rev. C* **19** (1979) 129-134.